Published by
NIGERIAN SOCIETY OF PHYSICAL SCIENCES
Available online @ https://journal.nsps.org.ng/index.php/jnsps

J. Nig. Soc. Phys. Sci. 8 (2026) 2959

Journal of the Nigerian Society of Physical Sciences

Effect of a moving thermal load in a modified couple stress medium with double porosity and hyperbolic two-temperature theory

Pragati[a], Rajneesh Kumar[b], Sachin Kaushal[a,*]

[a]*Department of Mathematics, School of Chemical Engineering and Physical Sciences, Lovely Professional University-144411 Phagwara, India*
[b]*Department of Mathematics, Kurukshetra University, Kurukshetra-136119 Haryana, India*

Abstract

In this study, a two-dimensional thermoelastic problem is investigated within the framework of modified couple stress theory (MCST) incorporating double porosity and governed by the hyperbolic two-temperature (HTT) model under the influence of a moving thermal source. The governing equations are reformulated in non-dimensional form and potential function techniques are employed to simplify the analysis. By applying normal mode analysis, closed-form analytical expressions are derived for key physical fields including displacement components, stress distributions, equilibrated stress tensors and temperature profiles. Numerical computations are carried out using MATLAB and the effects of the HTT model and the moving thermal load on the thermoelastic response are illustrated through graphical representations. Several particular cases of interest are examined to validate and interpret the model's behaviour under different physical conditions. The problem finds practical significance in areas such as microelectronics, civil engineering and biomedical device design particularly in areas involving thermal shock.

DOI:10.46481/jnsps.2026.2959

Keywords: Modified couple stress, Double porosity, Hyperbolic two temperature, Normal mode analysis

Article History :
Received: 23 May 2025
Received in revised form: 29 July 2025
Accepted for publication: 18 August 2025
Available online: 20 November 2025

Communicated by: P. Thakur

1. Introduction

Modern engineering materials and structures frequently consist of multiphase porous media where pores and microfractures develop due to natural degradation processes like erosion, corrosion, material fatigue or accidental impacts. These discontinuities can significantly alter the dynamic and mechanical behaviour of the structure. To capture these complexities, the double porosity theory has been introduced which accounts for two distinct void systems: one embedded within the matrix material and the other associated with microcracks or fractures. This theory has particular importance in modeling composite structures and naturally fractured rock formations.

Initial developments in this field were made by Wilson & Aifantis [1] who formulated a consolidation theory incorporating double porosity effects. This was later extended by Beskos & Aifantis [2] who provided analytical approaches to address boundary value problems in such materials. Further developments were carried out by Svanadze [3–7] who studied the response of elastic, viscoelastic and thermoelastic materials with double porosity. Scarpetta *et al.* [8] enriched this domain by establishing uniqueness theorems and deriving fundamental solutions within the thermoelastic double porosity context.

In parallel, advances in non-classical continuum mechanics have emerged. The couple stress theory introduced by Mindlin

*Corresponding author Tel. No.: +91-988-892-2806.
Email address: sachin_kuk@yahoo.co.in (Sachin Kaushal)

& Tiersten [9] incorporates additional material length scale parameters refining the classical elasticity framework and making it suitable for microscale analysis. A later enhancement, MCST proposed by Yang *et al.* [10] introduced a symmetric couple stress tensor by incorporating the balance of angular momentum, thereby improving the theoretical consistency.

Thermal modeling has also undergone significant refinement. Gurtin & Williams [11, 12] introduced a two-temperature theory (TT) by distinguishing between thermodynamic and conductive temperatures, even in scenarios devoid of external heat sources. This approach gained traction due to its capacity to resolve inconsistencies present in single-temperature models during time-dependent thermal processes. Subsequently, Youssef & El-Bary [13] extended this concept into HTT formulation allowing for finite-speed thermal wave propagation by modifying the classical relationship between the two temperatures.

In a complementary development, Tzou [14] formulated the dual phase lag (DPL) model, which introduces two separate time delays-one for the heat flux and another for the temperature gradient through a Taylor series expansion of the generalized heat conduction law leading to a more comprehensive thermal response model.

Recent investigations have focused on specialized implementations of these advanced theories. For example, Sharma & Khator [15, 16] explored applications related to renewable energy technologies while Gajroiya & Sikka [17] studied wave propagation at interfaces involving porothermoelastic and double porous materials. Sharma *et al.* [18] examined thermoelastic diffusion with temperature dependency and multiple phase lags. Mahato & Biswas [19] analyzed wave phenomena in nonlocal thermoelastic double porous media and Miglani *et al.* [20] investigated fractional-order models under DPL conditions. Additionally, Khatri *et al.* [21] studied thermal wave interactions in transversely isotropic double porous structures incorporating rotational and conductivity variation effects relevant to fiber-reinforced composites.

The present work focuses on the deformation characteristics of a modified couple stress thermoelastic double porous half-space exposed to a moving thermal source. The hyperbolic two-temperature theory is employed to accurately model the thermal field. Using the normal mode analysis method, analytical expressions are derived for displacement fields, stress tensors, equilibrated stresses and temperature profiles. The results are visualized graphically to elucidate the combined effects of the moving heat source and HTT model on the system's physical responses. Additionally, specific limiting cases are discussed to highlight notable special configurations and provide deeper insights into the physical behaviour of the medium.

2. Basic equations

Based on the formulations by Iesan & Quintanilla [22], Youssef *et al.* [13] and Kumar *et al.* [23], the governing equations for thermoelastic with HTT and double porosity without body forces, equilibrated forces and heat source are as

Stress-Strain-Temperature Relations:

$$t_{ij} = \lambda e_{rr}\delta_{ij} + 2\mu e_{ij} + b\delta_{ij}\phi^* + d\delta_{ij}\psi^* - \beta_1 T\delta_{ij}, \tag{1}$$

$$\sigma_i = b_1\psi^*_{,i} + \alpha_0\phi^*_{,i}, \tag{2}$$

$$m_{ij} = 2\alpha\chi_{ij}, \tag{3}$$

$$\chi_i = b_1\phi^*_{,i} + \gamma_0\psi^*_{,i}. \tag{4}$$

Governing equation of motion:

$$(\lambda + \mu + \frac{\alpha}{4}\Delta)\nabla\nabla.\mathbf{u} + (\mu - \frac{\alpha}{4}\Delta)(\nabla^2.\mathbf{u}) + b\nabla\phi^* + d\nabla\psi^* - \beta_1\nabla T = \rho\frac{\partial^2 u}{\partial t^2}, \tag{5}$$

Equilibrated stress equations of motion:

$$\alpha_0\nabla^2\phi^* + b_1\nabla^2\psi^* - b\nabla.\mathbf{u} - \alpha_1\phi^* - \alpha_3\psi^* + \gamma_1 T = \varphi_i\ddot{\phi}^*, \tag{6}$$

$$b_1\nabla^2\phi^* + \gamma_0\nabla^2\psi^* - d\nabla.\mathbf{u} - \alpha_3\phi^* - \alpha_2\psi^* + \gamma_2 T = \varphi_2\ddot{\psi}^*. \tag{7}$$

Governing equation for heat conduction:

$$K\left(1 + \tau_T\frac{\partial}{\partial t}\right)\nabla^2\phi = \left(1 + \tau_q\frac{\partial}{\partial t} + \frac{\tau_q^2}{2}\frac{\partial^2}{\partial^2 t}\right)[\gamma_1 T_0\dot{\phi}^* + \gamma_2 T_0\dot{\psi}^* + \beta_1 T_0\dot{e}_{kk} + \rho C_e\dot{T}]. \tag{8}$$

Here

$$\chi_{ij} = \frac{1}{2}(\omega_{i,j} + \omega_{j,i}), \quad \omega_i = \frac{1}{2}e_{ipq}u_{q,p}.$$

$\mathbf{u}$, λ, μ, α - couple stress parameter, Δ - Laplacian operator, ∇ - nabla (gradient) operator, T - temperature change, T_0 - reference temperature assumed to be such that $|T/T_0| \ll 1$, φ_1 and φ_2 - coefficients of equilibrated inertia, K- thermal conductivity, ρ - density, c_e- specific heat, b_1-coefficient describing the measure of mass diffusion, τ_T, τ_q - thermal relaxation times with τ_T, $\tau_q \geq 0$, $\beta_1 = (3\lambda + 2\mu)\alpha_t$, α_t - coefficients of linear thermal expansion, ψ^* and ϕ^* - volume fraction fields corresponding to fissures and pores respectively, $b, d, b_1, \gamma_0, \gamma_1, \gamma_2, \alpha_0, \alpha_1, \alpha_2, \alpha_3$ - constitutive coefficients, t_{ij} - stress tensor, δ_{ij} - Kronecker delta, e_{ijk} - alternate tensor, m_{ij} - couple stress tensor, χ_i - equilibrated stress corresponding to fissures, σ_i - equilibrated stress corresponding to pores respectively. The relation for HTT is given by [13]:

$$\ddot{T} = \ddot{\phi} - \beta^*\Delta\phi, \text{ where } T = \phi - a\Delta\phi, \tag{9}$$

and β^* is the hyperbolic two temperature parameter, a is the two temperature parameter (TT).

3. Statement and solution procedure

We consider a two-dimensional thermoelastic half-space $x_3 \geq 0$ modeled by modified couple stress theory with double porosity and hyperbolic two-temperature effects. The x_3 – axis points downward into the medium and the boundary at $x_3 = 0$ is exposed to a thermal load moving along the x_1 direction (Figure 1). All field variables depend on x_1, x_3 and t. Consequently, we write each quantity as follows:

$$\mathbf{u} = (u_1(x_1, x_3, t), 0, u_3(x_1, x_3, t)), T(x_1, x_3, t),$$

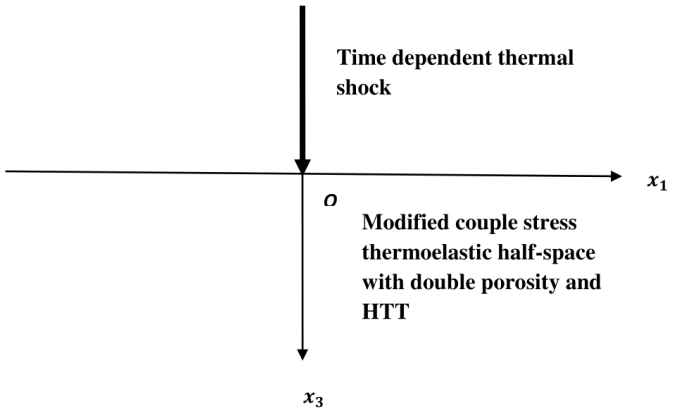

Figure 1: Geometry of the problem.

$$\phi^*(x_1, x_3, t), \psi^*(x_1, x_3, t). \tag{10}$$

Using equation (10) in equations (5)-(8), recast the following equations:

$$(\lambda+\mu)\frac{\partial e}{\partial x_1} + \mu\Delta u_1 + \frac{\alpha}{4}\Delta\left(\frac{\partial e}{\partial x_1} - \Delta u_1\right) + b\frac{\partial \phi^*}{\partial x_1} + d\frac{\partial \psi^*}{\partial x_1} - \beta_1\frac{\partial T}{\partial x_1} = \rho\frac{\partial^2 u_1}{\partial t^2}, \tag{11}$$

$$(\lambda+\mu)\frac{\partial e}{\partial x_3} + \mu\Delta u_3 + \frac{\alpha}{4}\Delta\left(\frac{\partial e}{\partial x_3} - \Delta u_3\right) + b\frac{\partial \phi^*}{\partial x_3} + d\frac{\partial \psi^*}{\partial x_3} - \beta_1\frac{\partial T}{\partial x_3} = \rho\frac{\partial^2 u_3}{\partial t^2}, \tag{12}$$

$$b_1\nabla^2\psi^* + \alpha_0\nabla^2\phi^* + \gamma_1 T - b\nabla\cdot\vec{u} - \alpha_3\psi^* - \alpha_1\phi^* = \varphi_1\frac{\partial^2\phi^*}{\partial t^2}, \tag{13}$$

$$b_1\nabla^2\phi^* + \gamma_0\nabla^2\psi^* - d\nabla\cdot\vec{u} - \alpha_3\phi^* - \alpha_2\psi^* + \gamma_2 T = \varphi_2\frac{\partial^2\psi^*}{\partial t^2}, \tag{14}$$

$$K\left[1+\tau_T\frac{\partial}{\partial t}\right]\nabla^2\phi = \left[1+\tau_q\frac{\partial}{\partial t}+\frac{\tau_q^2}{2}\frac{\partial^2}{\partial t^2}\right]\times \left[\gamma_1 T_0\dot{\phi}^* + \gamma_2 T_0\dot{\psi}^* + \beta_1 T_0\nabla\cdot\mathbf{u} + \rho C_e\dot{T}\right], \tag{15}$$

$$t_{33} = \lambda e + 2\mu\left(\frac{\partial u_3}{\partial x_3}\right) + b\phi^* + d\psi^* - \beta_1\frac{\partial T}{\partial x_3}, \tag{16}$$

$$t_{31} = \mu\left(\frac{\partial u_1}{\partial x_3} + \frac{\partial u_3}{\partial x_1}\right), \tag{17}$$

$$m_{32} = \frac{\alpha}{2}\frac{\partial}{\partial x_3}\left(\frac{\partial u_1}{\partial x_3} - \frac{\partial u_3}{\partial x_1}\right), \tag{18}$$

$$\sigma_3 = \alpha_0\frac{\partial\phi^*}{\partial x_3} + b_1\frac{\partial\psi^*}{\partial x_3}, \tag{19}$$

$$\chi_3 = b_1\frac{\partial\phi^*}{\partial x_3} + \gamma_0\frac{\partial\psi^*}{\partial x_3}. \tag{20}$$

The following dimensionless quantities are used:

$$x_i' = \frac{\omega^*}{c_1}x_i,\ \mathbf{u}' = \frac{\omega^*}{c_1}\mathbf{u},\ (t', \tau_q', \tau_T') = \omega^*(t, \tau_q, \tau_T),$$

$$\phi^{*'} = \frac{\varphi_1\omega^{*2}}{\alpha_1}\phi^*,\ \phi' = \frac{\phi}{T_0},$$

$$T' = \frac{T}{T_0},\ \psi^{*'} = \frac{\varphi_1\omega^{*2}}{\alpha_1}\psi^*,\ t_{ij}' = \frac{1}{\beta_1 T_0}t_{ij},\ \chi_i' = \left(\frac{c_1}{\alpha_0\omega^*}\right)\chi_i,$$

$$\sigma_i' = \left(\frac{c_1}{\alpha_0\omega^*}\right)\sigma_i, \tag{21}$$

$$m_{z\theta}' = \frac{\omega^*}{\beta_1 T_0 c_1}m_{z\theta},$$

where

$$\omega^* = \frac{\rho C_e c_1^2}{K},\ c_1^2 = \frac{\lambda+2\mu}{\rho}.$$

By utilizing equation (21), the system represented by equations (11)-(15) can be simplified to the following set of equations, with the primes omitted for clarity:

$$a_1\frac{\partial e}{\partial x_1} + a_2\Delta u_1 + a_3\Delta\left(\frac{\partial e}{\partial x_1} - \Delta u_1\right) + a_4\frac{\partial\phi^*}{\partial x_1} + a_5\frac{\partial\psi^*}{\partial x_1} - a_6\frac{\partial T}{\partial x_1} = \frac{\partial^2 u_1}{\partial t^2}, \tag{22}$$

$$a_1\frac{\partial e}{\partial x_3} + a_2\Delta u_3 + a_3\Delta\left(\frac{\partial e}{\partial x_3} - \Delta u_3\right) + a_4\frac{\partial\phi^*}{\partial x_3} + a_5\frac{\partial\psi^*}{\partial x_3} - a_6\frac{\partial T}{\partial x_3} = \frac{\partial^2 u_3}{\partial t^2}, \tag{23}$$

$$a_7\nabla^2\phi^* + a_8\nabla^2\psi^* - a_9 e - a_{10}\phi^* - a_{11}\psi^* + a_{12}T = \frac{\partial^2\phi^*}{\partial t^2}, \tag{24}$$

$$a_{13}\nabla^2\phi^* + a_{14}\nabla^2\psi^* - a_{15}e - a_{16}\phi^* - a_{17}\psi^* + a_{18}T = \frac{\partial^2\psi^*}{\partial t^2}, \tag{25}$$

$$a_{19}\left(1+\tau_T\frac{\partial}{\partial t}\right)\nabla^2\phi = \left[1+\tau_q\frac{\partial}{\partial t}+\frac{\tau_q^2}{2}\frac{\partial^2}{\partial t^2}\right]\left[a_{20}\frac{\partial e}{\partial t} + a_{21}\frac{\partial\phi^*}{\partial t} + a_{22}\frac{\partial\psi^*}{\partial t} + \frac{\partial T}{\partial t}\right], \tag{26}$$

where

$$a_1 = \frac{(\lambda+\mu)}{\rho c_1^2},\quad a_2 = \frac{\mu}{\rho c_1^2},\quad a_3 = \frac{a}{4}\frac{\omega^{*2}}{\rho c_1^4},$$
$$a_4 = \frac{b\alpha_1}{\varphi_1\rho c_1^2\omega^{*2}},\quad a_5 = \frac{d\alpha_1}{\varphi_1\omega^{*2}\rho c_1^2},\quad a_6 = \frac{\beta_1 T_0}{c_1^2\rho},$$
$$a_7 = \frac{a_0}{\varphi_1 c_1^2},\quad a_8 = \frac{b_1}{\varphi_1 c_1^2},\quad a_9 = \frac{b}{\alpha_1},$$
$$a_{10} = \frac{\alpha_1}{\varphi_1\omega^{*2}},\quad a_{11} = \frac{\alpha_3}{\varphi_1\omega^{*2}},\quad a_{12} = \frac{T_0\gamma_1}{\alpha_1},$$
$$a_{13} = \frac{b_1}{\varphi_2 c_1^2},\quad a_{14} = \frac{\gamma_0}{\varphi_2 c_1^2},\quad a_{15} = \frac{d\varphi_1}{\alpha_1\varphi_2},$$
$$a_{16} = \frac{\alpha_3}{\varphi_2\omega^{*2}},\quad a_{17} = \frac{\alpha_2}{\varphi_2\omega^{*2}},\quad a_{18} = \frac{\gamma_2 T_0\varphi_1}{\alpha_1\varphi_2},$$
$$a_{19} = \frac{k\omega^*}{\rho C_e c_1^2},\quad a_{20} = \frac{\beta_1}{\rho C_e},\quad a_{21} = \frac{\gamma_1\alpha_1}{\varphi_1\omega^{*2}\rho C_e},$$

$$a_{22} = \frac{\gamma_2\alpha_1}{\rho C_e \varphi_1 \omega^{*2}}.$$

The displacement components $u_1(x_1, x_3, t)$ and $u_3(x_1, x_3, t)$ relate to scalar potentials $\phi_1(x_1, x_3, t)$ and $\psi_1(x_1, x_3, t)$ in dimensionless form as

$$u_1 = \frac{\partial\phi_1}{\partial x_1} - \frac{\partial\psi_1}{\partial x_3}, \quad u_3 = \frac{\partial\phi_1}{\partial x_3} + \frac{\partial\psi_1}{\partial x_1}. \tag{27}$$

With the aid of (27), equations (22)-(26) yield:

$$\left[(a_1 + a_2)\Delta - \frac{\partial^2}{\partial t^2}\right]\phi_1 + a_4\phi^* + a_5\psi^* - a_6 T = 0, \tag{28}$$

$$-a_9\Delta\phi_1 + \left(a_7\Delta - a_{10} - \frac{\partial^2}{\partial t^2}\right)\phi^* + (a_8\Delta - a_{11})\psi^* + a_{12}T = 0, \tag{29}$$

$$-a_{15}\Delta\phi_1 + (a_{13}\Delta - a_{16})\phi^* + \left(a_{14}\Delta - a_{17} - \frac{\partial^2}{\partial t^2}\right)\psi^* + a_{18}T = 0, \tag{30}$$

$$a_{19}\left(1 + \tau_T\frac{\partial}{\partial t}\right)\Delta\phi = \left[1 + \tau_q\frac{\partial}{\partial t} + \frac{\tau_q^2}{2}\frac{\partial^2}{\partial t^2}\right]\left[a_{20}\frac{\partial(\Delta\phi_1)}{\partial t} + a_{21}\frac{\partial\phi^*}{\partial t} + a_{22}\frac{\partial\psi^*}{\partial t} + \frac{\partial T}{\partial t}\right], \tag{31}$$

$$\left[a_2\Delta + a_3\Delta^2 + \frac{\partial^2}{\partial t^2}\right]\psi_1 = 0. \tag{32}$$

We assume the solution of equations (28)-(32) as:

$$(\phi_1, \psi_1, \phi^*, \psi^*, \phi) = (\hat{\phi}_1, \hat{\psi}_1, \hat{\phi}^*, \hat{\psi}^*, \hat{\phi})e^{ik(x_1 - ct)}, \tag{33}$$

where $\omega = kc$, k is the wave number and c is the phase velocity.

Using equation (33) in equation (9) determine:

$$\hat{T} = [1 + \zeta^*(D^2 - k^2)]\hat{\phi}, \tag{34}$$

where

$$\zeta^* = \begin{cases} \dfrac{\beta^*}{\omega^{*2}}, & \text{HTT} \\ a, & \text{TT} \\ 0, & \text{1T}. \end{cases}$$

$D = \dfrac{d}{dx_3}$, $1T$ indicates one temperature.

Inserting equation (33) in equations (28)-(32) and with aid of equation (34) gives:

$$\begin{bmatrix} a_{23}D^2 - a_{24} & a_4 & a_5 & a_{25} - a_{26}D^2 \\ -a_9D^2 + a_{29} & a_7D^2 + a_{30} & a_8D^2 + a_{31} & a_{32}D^2 + a_{33} \\ -a_{15}D^2 + a_{34} & a_{13}D^2 + a_{35} & a_{14}D^2 + a_{36} & a_{37}D^2 + a_{38} \\ -a_{39}D^2 + a_{40} & -a_{41} & -a_{42} & a_{43}D^2 + a_{44} \end{bmatrix}\begin{bmatrix} \hat{\phi}_1 \\ \hat{\phi}^* \\ \hat{\psi}^* \\ \hat{\phi} \end{bmatrix} = 0 \tag{35}$$

$$[a_3D^4 + a_{27}D^2 + a_{28}]\hat{\psi}_1 = 0, \tag{36}$$

where

$$\begin{aligned}
a_{23} &= a_1 + a_2, \\
a_{24} &= a_{23}k^2 + \omega^2, \\
a_{25} &= a_6(\zeta^*k^2 - 1), \\
a_{26} &= a_6\zeta^*, \\
a_{27} &= -(a_2 + 2a_3k^2), \\
a_{28} &= a_3k^4 + a_2k^2 - \omega^2, \\
a_{29} &= a_9k^2, \\
a_{30} &= -a_7k^2 - a_{10} + \omega^2, \\
a_{31} &= -a_8k^2 - a_{11}, \\
a_{32} &= a_{12}\zeta^*, \\
a_{33} &= -a_{12}(\zeta^*k^2 - 1), \\
a_{34} &= a_{15}k^2, \\
a_{35} &= -a_{13}k^2 - a_{16}, \\
a_{36} &= -a_{14}k^2 - a_{17} + \omega^2, \\
a_{37} &= a_{18}\zeta^*, \\
a_{38} &= -a_{18}(\zeta^*k^2 - 1), \\
a_{39} &= a_{20}\tau_q^0, \\
a_{40} &= a_{39}k^2, \\
a_{41} &= a_{21}\tau_q^0, \\
a_{42} &= a_{22}\tau_q^0, \\
a_{43} &= a_{19}\tau_T^0 - \tau_q^0\zeta^*, \\
a_{44} &= \tau_q^0(\zeta^*k^2 - 1) - a_{19}\tau_T^0k^2, \\
\tau_T^0 &= (1 + \tau_T(-i\omega)), \\
\tau_q^0 &= (-i\omega)\left[1 + \tau_q(-i\omega) + \frac{\tau_q^2}{2}(-i\omega)^2\right].
\end{aligned}$$

On solving equation (35), we obtain:

$$(A_1D^8 + A_2D^6 + A_3D^4 + A_4D^2 + A_5)(\hat{\phi}_1, \hat{\phi}^*, \hat{\psi}^*, \hat{\phi}) = 0, \tag{37}$$

where A_1, A_2, A_3, A_4, A_5 are given in Appendix I.

The analytical solutions for equations (36) and (37) are obtained and presented below:

$$(\widehat{\phi}_1, \hat{\phi}^*, \hat{\psi}^*, \hat{\phi}) = \sum_{j=1}^{4}(1, R_j^*, S_j^*, U_j^*)A_je^{-m_jx_3}, \tag{38}$$

$$\psi_1' = \sum_{j=5}^{6}A_je^{-m_jx_3}, \tag{39}$$

and $m_j (j = 1, 2, ..., 6)$ are the roots of equations:

$$(A_1D^8 + A_2D^6 + A_3D^4 + A_4D^2 + A_5) = 0, \tag{40}$$

$$(a_3D^4 + a_{27}D^2 + a_{28}) = 0, \tag{41}$$

and the coupling constants R_j^*, S_j^* and U_j^* are given in the Appendix I.

4. Boundary restrictions

A moving thermal shock is applied to the boundary half-surface $x_3 = 0$ along with the vanishing of normal stress, tangential stress and equilibrated stresses. According, the boundary conditions imposed on the surface $x_3 = 0$ are expressed as follows:

$$t_{33} = 0, \quad t_{31} = 0, \quad m_{32} = 0, \sigma_3 = 0, \chi_3 = 0,$$
$$\phi = F_{20} V_0 e^{i(k_1 x - \omega t)}, \tag{42}$$

where F_{20} is the intensity of the load applied and V_0 is the velocity of applied load.

Also,

$$t_{33} = c_{11} e + 2c_{12}\left(\frac{\partial u_3}{\partial x_3}\right) + c_{13}\phi^* + c_{14}\psi^* - \left(1 + \zeta^* \Delta\right)\phi, \tag{43}$$

$$t_{31} = c_{12}\left(\frac{\partial u_1}{\partial x_3} + \frac{\partial u_3}{\partial x_1}\right) - c_{15}\left(\frac{\partial^2}{\partial x_1^2} + \frac{\partial^2}{\partial x_3^2}\right)\left(\frac{\partial u_1}{\partial x_3} - \frac{\partial u_3}{\partial x_1}\right), \tag{44}$$

$$m_{32} = 2c_{15}\frac{\partial}{\partial x_3}\left(\frac{\partial u_1}{\partial x_3} - \frac{\partial u_3}{\partial x_1}\right), \tag{45}$$

$$\sigma_3 = c_{16}\frac{\partial \phi^*}{\partial x_3} - c_{17}\frac{\partial \psi^*}{\partial x_3}, \tag{46}$$

$$\chi_3 = c_{17}\frac{\partial \phi^*}{\partial x_3} - c_{18}\frac{\partial \psi^*}{\partial x_3}. \tag{47}$$

where $c_{11}, c_{12}, c_{13}, c_{14}, c_{15}, c_{16}, c_{17}, c_{18}$ are given appendix II.

By substituting the expressions for $\phi, \psi_1, \phi^*, \psi^*, \phi_1$ from equations (38) and (39) into the boundary conditions specified in equation (42) and utilizing equations (43) through (47) along with equation (27), the resulting formulations for the stress components and temperature distribution are derived as follows:

$$\widetilde{t_{33}} = \frac{1}{\Delta}\Big[Q_1^0\Delta_1 e^{-m_1 x_3} + Q_2^0\Delta_2 e^{-m_2 x_3} + Q_3^0\Delta_3 e^{-m_3 x_3} + Q_4^0\Delta_4 e^{-m_4 x_3} + Q_5^0\Delta_5 e^{-m_5 x_3} + Q_6^0\Delta_6 e^{-m_6 x_3}\Big], \tag{48}$$

$$\widetilde{t_{31}} = \frac{1}{\Delta}\Big[H_1^0\Delta_1 e^{-m_1 x_3} + H_2^0\Delta_2 e^{-m_2 x_3} + H_3^0\Delta_3 e^{-m_3 x_3} + H_4^0\Delta_4 e^{-m_4 x_3} + H_5^0\Delta_5 e^{-m_5 x_3} + H_6^0\Delta_6 e^{-m_6 x_3}\Big], \tag{49}$$

$$\widetilde{m}_{32} = \frac{1}{\Delta}\Big[M_5^0\Delta_5 e^{-m_3 x_3} + M_6^0\Delta_6 e^{-m_6 x_3}\Big], \tag{50}$$

$$\widetilde{\sigma}3 = \frac{1}{\Delta}\Big[N_1^0\Delta_1 e^{-m_1 x_3} + N_2^0\Delta_2 e^{-m_2 x_3} + N_3^0\Delta_3 e^{-m_3 x_3} + N_4^0\Delta_4 e^{-m_4 x_3}\Big], \tag{51}$$

$$\widetilde{\chi}_3 = \frac{1}{\Delta}\Big[E_1^0\Delta_1 e^{-m_1 x_3} + E_2^0\Delta_2 e^{-m_2 x_3} + E_3^0\Delta_3 e^{-m_3 x_3} + E_4^0\Delta_4 e^{-m_4 x_3}\Big], \tag{52}$$

$$\widetilde{\phi} = \frac{1}{\Delta}\Big[L_1^0\Delta_1 e^{-m_1 x_3} + L_2^0\Delta_2 e^{-m_2 x_3} + L_3^0\Delta_3 e^{-m_3 x_3} + L_4^0\Delta_4 e^{-m_4 x_3}\Big]. \tag{53}$$

where

$$\Delta = \begin{vmatrix} Q_1^0 & Q_2^0 & Q_3^0 & Q_4^0 & Q_5^0 & Q_6^0 \\ H_1^0 & H_2^0 & H_3^0 & H_4^0 & H_5^0 & H_6^0 \\ 0 & 0 & 0 & 0 & M_S^0 & M_6^0 \\ N_1^0 & N_2^0 & N_3^0 & N_4^0 & 0 & 0 \\ E_1^0 & E_2^0 & E_3^0 & E_4^0 & 0 & 0 \\ L_1^0 & L_2^0 & L_3^0 & L_4^0 & 0 & 0 \end{vmatrix}. \tag{54}$$

$\Delta_i (i = 1 - 6)$ are obtained by replacing j^{th} column of equation (54) with $[0, 0, 0, 0, 0, F_{20} V_0]^{tr}$ where $Q_j^0, H_j^0 (j = 1 - 6), M_j^0 (j = 5, 6), N_j^0, E_j^0, L_j^0 (j = 1 - 4)$ are given in the Appendix III.

Particular cases are obtained as:

(i) If $\zeta^* \to a$ in the equations (48) - (53), we obtained the corresponding expressions for MCST with two temperature and double porous medium.

(ii) If $d = b_1 = \gamma_o = \alpha_2 = \alpha_3 = \gamma_2 = 0$ in the equations (48) - (53), yield the corresponding expression for MCST with HTT and single porous material.

(iii) $\alpha_0 = b = b_1 = \alpha_1 = \alpha_2 = \alpha_3 = \gamma_1 = \gamma_2 = d = \gamma_o = 0$ in the equations (48) - (53), determine the resulting quantities for MCST with HTT.

5. Numerical results and discussion

Following Sherief and Saleh [24], copper is selected as the material for numerical analysis, with the corresponding thermophysical parameters defined as follow:

$$\lambda = 776 \times 10^7\,\mathrm{kgm^{-1}s^{-2}}, \quad \mu = 386 \times 10^7\,\mathrm{kgm^{-1}s^{-2}},$$
$$T_0 = 0.293 \times 10^3\,\mathrm{K}, C_e = 383.1\,\mathrm{Jkg^{-1}K^{-1}},$$
$$\alpha_t = 1.78 \times 10^{-5}\,\mathrm{K^{-1}}, \quad \rho = 8954\,\mathrm{kgm^{-3}},$$
$$K = 386\,\mathrm{Wm^{-1}K^{-1}}, \quad \alpha = 5 \times 10^{-2}\,\mathrm{kgms^{-2}},$$
$$t = 0.01\mathrm{s}, \quad \tau_T = 0.4\mathrm{s}, \quad \tau_q = 0.6\mathrm{s}.$$

and double porous parameters are taken as:

$$\alpha_0 = 1.3 \times 10^{-5}\,\mathrm{N}, \quad \alpha_1 = 2.3 \times 10^{10}\,\mathrm{Nm^{-2}},$$
$$\alpha_2 = 2.4 \times 10^{10}\,\mathrm{Nm^{-2}}, \quad \alpha_3 = 2.5 \times 10^{10}\,\mathrm{Nm^{-2}},$$
$$\gamma_0 = 1.1 \times 10^{-5}\,\mathrm{N}, \quad \gamma_1 = 0.16 \times 10^5\,\mathrm{Nm^{-2}},$$
$$\gamma_2 = 219 \times 10^2\,\mathrm{Nm^{-2}}, \quad b_1 = 0.12 \times 10^{-5}\,\mathrm{N},$$
$$d = 1 \times 10^9\,\mathrm{Nm^{-2}}, \quad b = 0.9 \times 10^{10}\,\mathrm{Nm^{-2}},$$
$$\varphi_1 = 0.1456 \times 10^{-12}\,\mathrm{Nm^{-2}s^2}, \quad \varphi_2 = 0.1546 \times 10^{-12}\,\mathrm{Nm^{-2}s^2}.$$

The software MATLAB has been used to find the value of normal stress t_{33}, tangential stress t_{31}, tangential couple stress m_{32}, conductive temperature ϕ and equilibrated stress σ_3. The variations of these values with respect to distance x_1 have been shown in Figures 2 - 11 respectively. In Figures 2 - 6, solid line (—) corresponds to $v_0 = 0.5$, dash line (...) corresponds to $v_0 = 0.3$ and dotted line (–*–*–) corresponds to $v_0 = 0.1$. In Figures 7 - 11, solid line (—) corresponds to MCSTDH,

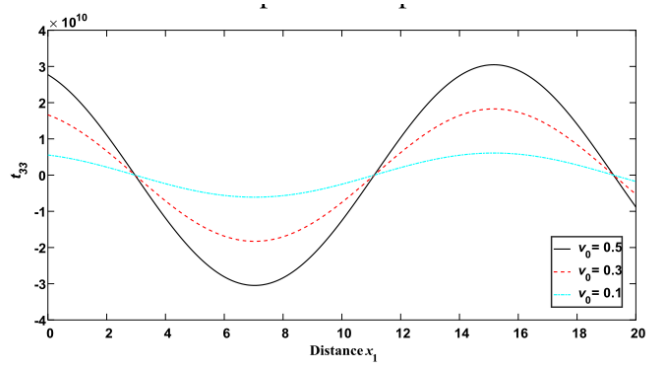

Figure 2: Variation of normal stress t_{33} with x_1 for different thermal source velocities v_0.

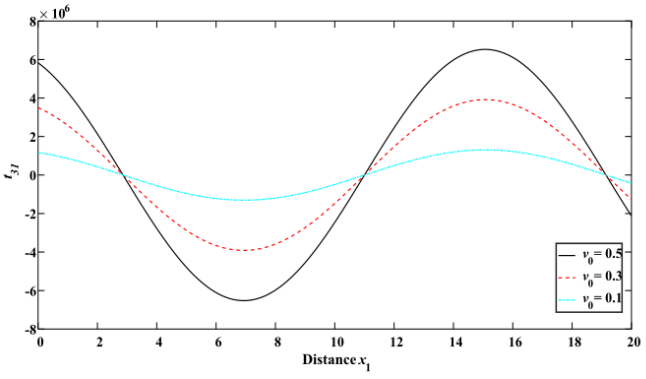

Figure 3: Variation of tangential stress t_{31} with x_i for different thermal source velocities v_0.

dash line (...) corresponds to MCSTDT and dotted line (–*–*–) corresponds to MCSTDO. MCSTDH denotes modified couple stress theory with double porous for hyperbolic two temperature (HTT), MCSTDT denotes modified couple stress theory with double porous for two temperature (TT) and MCSTDO denotes modified couple stress theory with porous for one temperature (1T).

Figure 2 illustrates the variation normal stress t_{33} with respect to distance x_1. As seen in the plot for a higher value of $v_0 = 0.5, t_{33}$ exhibits the largest amplitude and most pronounced oscillations, indicating HTT effect and higher stress sensitivity. With a moderate value of $v_0 = 0.3$, the amplitude of t_{33} decreases and the waveform becomes smoother whereas, for the lowest value $v_0 = 0.1$, the stress response is the least dynamic with small amplitude and damped oscillation.

Figure 3 shows the variation of t_{31}. For $v_0 = 0.5, t_{31}$ displays the largest amplitude and most pronounced oscillations. As v_0 decreases to 0.3, the amplitude reduces and the waveform becomes smoother, suggesting a moderate nonlocal influence. With $v_0 = 0.1$, the variation of t t_{31} is the most subdued showing low amplitude and flatter oscillations.

Figure 4 demonstrates the variation of m_{32} with respect to distance x_1. For $v_0 = 0.5, m_{32}$ exhibits large amplitude and sharp oscillations. As v_0 decreases to 0.3, the amplitude of m_{32} reduces and the oscillations become smoother oscillations.

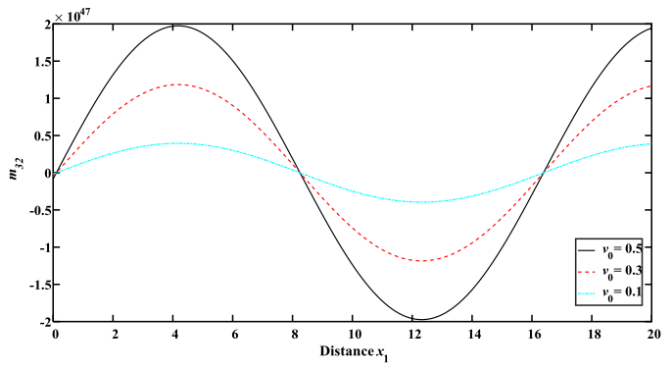

Figure 4: Variation of tangential couple stress m_{32} with x_1 for different thermal source velocities v_0.

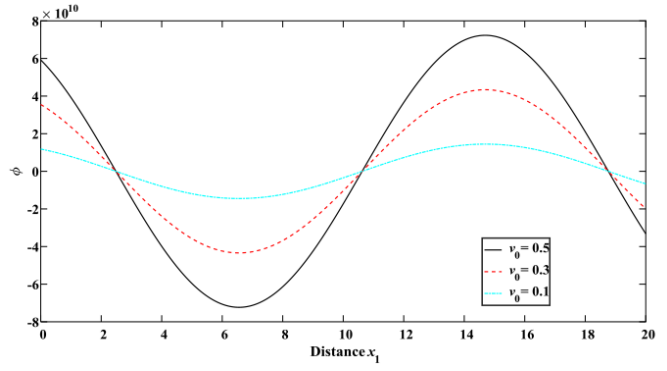

Figure 5: Variation of conductive temperature ϕ with x_1 for different thermal source velocities v_0.

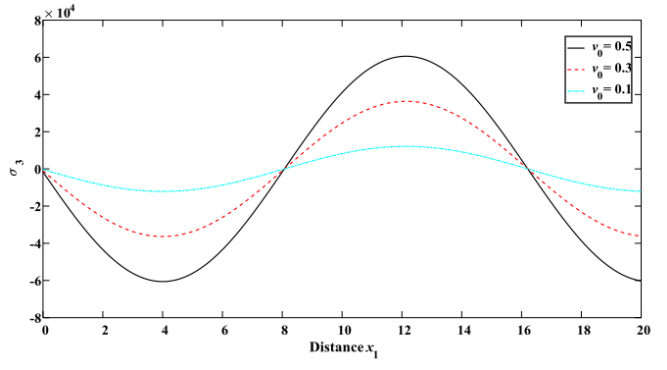

Figure 6: Variation of equilibrated stress σ_3 with x_1 for different thermal source velocities v_0.

Figure 5 shows the variation of ϕ with respect to distance x_1. For $v_0 = 0.5, \phi$ shows large amplitude and distinct oscillatory behaviour. v_0 decreases to 0.3, the amplitude of ϕ reduces and the waveform becomes smoother, whereas at $v_0 = 0.1, \phi$ is significantly damped with a flatter profile and minimal variation.

Figure 6 displays the variation of σ_3 with respect to distance x_1. For $v_0 = 0.5$, σ_3 exhibits the largest amplitude and most pronounced oscillations. When $v_0 = 0.3$ (red dashed line), the amplitude of σ_3 decreases, and for $v_0 = 0.1$, σ_3 shows the

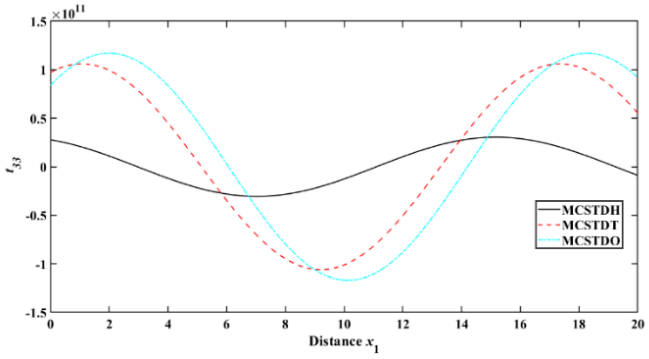

Figure 7: Variation of normal stress t_{33} with x_1 for HTT, TT, 1T.

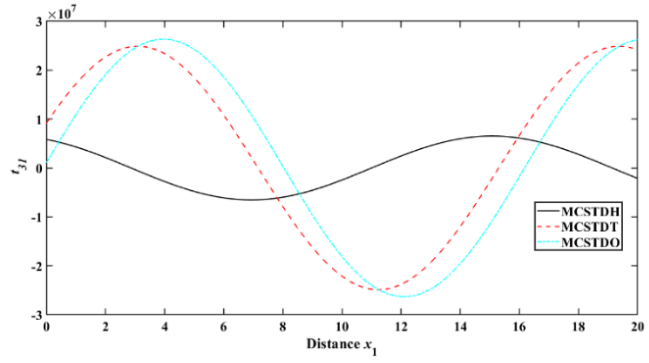

Figure 8: Variation of tangential stress t_{31} with x_1 for HTT, TT, 1T.

smallest amplitude and the flattest variation.

Figure 7 demonstrates the variation of t_{33} with respect to distance x_1. In the MCSTDH model, t_{33} varies smoothly with a low amplitude and long wavelength. For the MCSTDT model, t_{33} exhibits moderate oscillations with increased amplitude and a slightly shorter wavelength whereas, in the MCSTDO model, t_{33} shows the most significant variation characterized by high amplitude and rapid oscillations.

Figure 8 displays variation of t_{31} with respect to distance x_1. For MCSTDH, t_{31} varies gradually with low amplitude and a broad wavelength. In the MCSTDT model, t_{31} shows a more pronounced oscillation with increased amplitude and shorter wavelength whereas for MCSTDO model, t_{31} exhibits the highest amplitude and most rapid oscillations.

Figure 9 depicts variation of m_{32} with respect to x_1. In the MCSTDH model, m_{32} exhibits a prominent sinusoidal pattern with large amplitude. In contrast, both MCSTDT and MCSTDO models show significantly reduced amplitude with much flatter variations.

Figure 10 shows the variation of ϕ with respect to x_1. For MCSTDH, ϕ exhibits a strong sinusoidal variation with large amplitude. In contrast, both the MCSTDT and MCSTDO models display much lower amplitudes with smoother and less pronounced oscillations.

Figure 11 demonstrates variation of σ_3 with respect x_1.

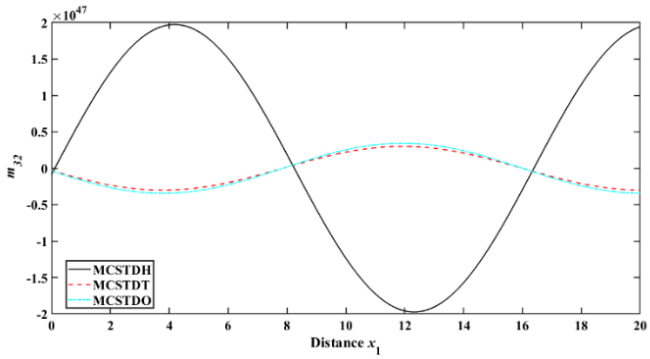

Figure 9: Variation of tangential couple stress m_{32} with x_1 for HTT, TT, 1T.

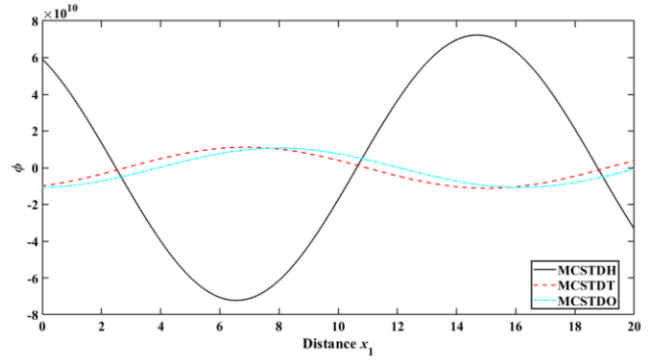

Figure 10: Variation of conductive temperature ϕ with x_1 for HTT, TT, 1T.

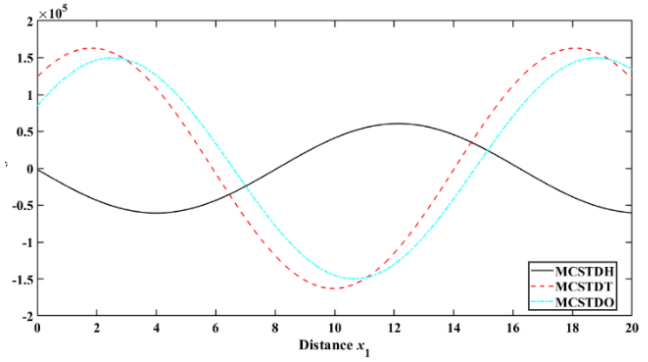

Figure 11: Variation of equilibrated stress σ_3 with x_1 for HTT, TT, 1T.

For MCSTDH, σ_3 exhibits a smooth low-amplitude response with broader wavelength. In comparison, the MCSTDT model shows a more pronounced oscillatory behaviour with higher amplitude and shorter wavelength. The MCSTDO model displays similar behaviour to MCSTDT but with slightly higher frequency oscillations and comparable amplitude.

6. Conclusions

In this study, the deformation behaviour of a thermoelastic half-space incorporating modified couple stress theory, double porosity and the hyperbolic two-temperature (HTT) model under a moving thermal load has been analyzed. The normal mode analysis method was employed to derive solutions for physical field quantities such as displacements, stresses and temperature distributions. The effects of the moving thermal load and HTT model have been illustrated graphically. The numerical results reveal that the magnitudes of normal and tangential stresses are significantly higher at the initial and final positions for increased values of thermal wave velocity. Additionally, tangential couple stress and equilibrated stress exhibit opposite trends across all cases considered. The variation of HTT differs notably from both the classical one-temperature (1T) and two-temperature (TT) models, especially in terms of tangential couple stress and conductive temperature. It is observed that HTT both amplifies and diminishes the magnitudes of normal and tangential stresses, depending on position while the conductive temperature shows reverse behaviour in HTT and 1T models as the distance increases.

The study provides new insights into how microscale structure and advanced heat conduction models, such as the hyperbolic two-temperature theory, influence the thermo-mechanical response of copper-based porous media under dynamic thermal loading. These findings contribute to improved design and reliability of copper components in thermal management systems, electronic packaging and bioMEMS applications.

Data availability

The data supporting the findings of this study are available from the corresponding author upon reasonable request.

Acknowledgment

The authors declare that no external funding was received for the conduct of this study.

References

[1] R. K. Wilson & E. C. Aifantis, "On the theory of consolidation with double porosity", International Journal of Engineering Science **20** (1982) 1009. https://doi.org/10.1016/0020-7225(82)90036-2.

[2] D. E. Beskos & E. C. Aifantis, "On the theory of consolidation with double porosity II", International Journal of Engineering Science **24** (1986) 1697. https://doi.org/10.1016/0020-7225(86)90076-5.

[3] M. Svanadze, "Fundamental solution in the theory of consolidation with double porosity", Journal of Mechanical Behavior of Materials **16** (2005) 123. http://dx.doi.org/10.1515/JMBM.2005.16.1-2.123.

[4] M. Svanadze, "Dynamical problems on the theory of elasticity for solids with double porosity", Proceedings in Applied Mathematics and Mechanics **10** (2010) 209. http://dx.doi.org/10.1002/pamm.201010147.

[5] M. Svanadze, "Plane waves and boundary value problems in the theory of elasticity for solids with double porosity", Acta Applicandae Mathematicae **122** (2012) 461. https://doi.org/10.1007/s10440-012-9756-5.

[6] M. Svanadze, "On the theory of viscoelasticity for materials with double porosity", Discrete and Continuous Dynamical Systems-B **19** (2014) 2335. https://doi.org/10.3934/dcdsb.2014.19.2335.

[7] M. Svanadze, "Uniqueness theorems in the theory of thermoelasticity for solids with double porosity", Meccanica **49** (2014) 2099. https://doi.org/10.1007/s11012-014-9876-2.

[8] E. Scarpetta, M. Svanadze & V. Zampoli, "Fundamental solutions in the theory of thermoelasticity for solids with double porosity", Journal of Thermal Stresses **37** (2014) 727. https://doi.org/10.1080/01495739.2014.885337.

[9] R. D. Mindlin & H. F. Tiersten, "Effects of couple-stresses in linear elasticity", Archive for Rational Mechanics and Analysis **11** (1962) 415. https://doi.org/10.1007/BF00253946.

[10] F. Yang, A. C. M. Chong, D. C. C. Lam & P. Tong, "Couple stress based strain gradient theory for elasticity", International Journal of Solids and Structures **39** (2002) 2731. https://doi.org/10.1016/S0020-7683(02)00152-X.

[11] M. E. Gurtin & W. O. Williams, "On the Clausius-Duhem inequality", Journal of Applied Mathematics and Physics (ZAMP) **17** (1966) 626. https://doi.org/10.1007/BF01597243.

[12] M. E. Gurtin & W. O. Williams, "An axiomatic foundation for continuum thermodynamics", Archive for Rational Mechanics and Analysis **26** (1967) 83. http://dx.doi.org/10.1007/BF00285676.

[13] H. M. Youssef & A. A. El-Bary, "Theory of hyperbolic two temperature generalized thermoelasticity", Material Physics and Mechanics **40** (2018) 158. https://doi.org/10.18720/MPM.4022018_4.

[14] D. Y. Tzou, "A unified field approach for heat conduction from macro-to micro-scales", Journal of Heat Transfer **117** (1995) 8. https://doi.org/10.1115/1.2822329.

[15] S. Sharma & S. Khator, "Power generation planning with reserve dispatch and weather uncertainties including penetration of renewable sources", International Journal of Smart Grid and Clean Energy **1** (2021) 292. https://doi.org/10.12720/sgce.10.4.292-303.

[16] S. Sharma & S. Khator, "Micro-grid planning with aggregator's role in the renewable inclusive prosumer market", Journal of Power and Energy Engineering **10** (2022) 47. https://doi.org/10.4236/jpee.2022.104004.

[17] K. Gajroiya & J. S. Sikka, "Reflection and transmission of plane waves from the interface of a porothermoelastic solid and a double porosity solid", European Physical Journal Plus **139** (2024) 468. https://doi.org/10.1140/epjp/s13360-024-05215-x.

[18] S. Sharma, S. Devi, R. Kumar & M. Marin, "Examining basic theorems and plane waves in the context of thermoelastic diffusion using a multi-phase-lag model with temperature dependence", Mechanics of Advanced Materials and Structures **32** (2024) 1. https://doi.org/10.1080/15376494.2024.2370523.

[19] C. S. Mahato & S. Biswas, "Thermomechanical interactions in nonlocal thermoelastic medium with double porosity structure", Mechanics of Time-Dependent Materials **28** (2024) 1073. https://doi.org/10.1007/s11043-024-09669-5.

[20] A. Miglani, R. Kumar, A. Kaur & M. Karla, "Axisymmetric deformation of a circular plate of double-porous fractional order thermoelastic medium with dual-phase-lag", Acta Mechanica **235** (2024) 7263. https://doi.org/10.1007/s00707-024-04092-w.

[21] M. Khatri, S. Deswal & K. K. Kalkal, "Fiber-reinforced material in a double porous transversely isotropic medium with rotation and variable thermal conductivity", Acta Mechanica **236** (2025) 1819. https://doi.org/10.1007/s00707-025-04238-4.

[22] D. Iesan & R. Quintanilla, "On a theory of thermoelastic materials with a double porosity structure", Journal of Thermal Stresses **37** (2014) 1017. http://dx.doi.org/10.1080/01495739.2014.914776.

[23] R. Kumar, S. Devi & V. Sharma, "Axisymmetric problem of thick circular plate with heat source in modified couple stress theory", Journal of Solid Mechanics **9** (2017) 157. https://oiccpress.com/jsm/article/view/12587.

[24] H. H. Sherief & H. Saleh, "A half-space problem in the theory of generalized thermoelastic diffusion", International Journal of Solids and Structures **42** (2005) 4484. https://doi.org/10.1016/j.ijsolstr.2005.01.001.

Appendix I

$$
\begin{aligned}
A_1 &= a_7a_{14}a_{23}a_{43} - a_8a_{13}a_{23}a_{43} + a_8a_{13}a_{26}a_{39},\\
A_2 &= a_7a_{23}(a_{36}a_{43} + a_{14}a_{44} + a_{37}a_{42}) + a_{23}a_{30}a_{14}a_{43}\\
&\quad - a_8a_{23}(a_{35}a_{43} + a_{13}a_{44} + a_{37}a_{41}) - a_{23}a_{31}a_{13}a_{43}\\
&\quad + a_{23}a_{32}(a_{14}a_{41} - a_{13}a_{42}) + a_{43}(a_8a_{24}a_{13} - a_7a_{14}a_{24} + a_4a_9a_{14})\\
&\quad + a_8a_4(a_{37}a_{39} - a_{15}a_{43}) - a_4a_{14}a_{32}a_{39} - a_5a_9a_{13}a_{43}\\
&\quad + a_5a_7(a_{15}a_{43} - a_{37}a_{39}) + a_5a_{13}a_{32}a_{39} - a_9a_{26}(a_{14}a_{41} - a_{13}a_{42})\\
&\quad - a_7a_{26}(a_{15}a_{42} + a_{14}a_{39} + a_{36}a_{39} - a_{14}a_{40})\\
&\quad + a_8a_{26}(a_{15}a_{41} + a_{35}a_{39} - a_{13}a_{40}) - a_8a_{25}a_{13}a_{39} + a_{26}a_{31}a_{13}a_{39},\\
A_3 &= a_7a_{23}(a_{36}a_{44} + a_{38}a_{42}) + a_{23}a_{30}(a_{36}a_{43} + a_{14}a_{44} + a_{37}a_{42})\\
&\quad - a_{23}a_8(a_{35}a_{44} + a_{38}a_{41}) - a_{23}a_{31}(a_{35}a_{43} + a_{13}a_{44} + a_{37}a_{41})\\
&\quad + a_{23}a_{29}(a_{36}a_{41} - a_{35}a_{42}) + a_{23}a_{33}(a_{14}a_{41} - a_{13}a_{42})\\
&\quad - a_7a_{24}(a_{36}a_{43} + a_{14}a_{44} + a_{37}a_{42}) - a_{25}a_{30}a_{14}a_{43}\\
&\quad + a_8a_{24}(a_{35}a_{43} + a_{13}a_{44} + a_{37}a_{41}) + a_{24}a_{31}a_{13}a_{43}\\
&\quad - a_{24}a_{32}(a_{14}a_{41} - a_{13}a_{42}) + a_4a_9(a_{36}a_{43} + a_{14}a_{44} + a_{37}a_{42})\\
&\quad - a_4a_{29}a_{14}a_{43} + a_8a_4(a_{34}a_{43} - a_{15}a_{44} + a_{38}a_{39} - a_{37}a_{40})\\
&\quad + a_4a_{31}(a_{37}a_{39} - a_{15}a_{43}) - a_4a_{32}(a_{15}a_{42} + a_{36}a_{39} - a_{14}a_{40})\\
&\quad - a_4a_{14}a_{33}a_{39} - a_5a_9(a_{35}a_{43} + a_{13}a_{44} + a_{38}a_{42}) + a_5a_{30}a_{13}a_{43}\\
&\quad - a_5a_7(a_{34}a_{43} - a_{15}a_{44} + a_{38}a_{39} - a_{37}a_{40}) - a_5a_{30}(a_{37}a_{39} - a_{15}a_{43})\\
&\quad + a_5a_{32}(a_{15}a_{41} + a_{35}a_{39} - a_{13}a_{40}) + a_5a_{13}a_{33}a_{39}\\
&\quad - a_9a_{26}(a_{36}a_{41} - a_{35}a_{42}) + a_9a_{25}(a_{14}a_{41} - a_{13}a_{42})\\
&\quad + a_{20}a_{26}(a_{14}a_{41} - a_{13}a_{42}) + a_7a_{26}(a_{34}a_{42} + a_{36}a_{40})\\
&\quad + a_7a_{25}(a_{15}a_{42} + a_{14}a_{39} + a_{36}a_{39} - a_{14}a_{40})\\
&\quad - a_{26}a_{30}(a_{15}a_{42} + a_{14}a_{39} + a_{36}a_{39} - a_{14}a_{40})\\
&\quad - a_8a_{26}(a_{34}a_{41} + a_{35}a_{40}) - a_8a_{25}(a_{15}a_{41} + a_{35}a_{39} - a_{13}a_{40})\\
&\quad + a_{26}a_{31}(a_{15}a_{41} + a_{36}a_{40} - a_{13}a_{40}) - a_{25}a_{31}a_{13}a_{39},\\
A_4 &= a_{30}a_{23}(a_{36}a_{44} + a_{38}a_{42}) - a_{23}a_{31}(a_{35}a_{44} + a_{38}a_{41})\\
&\quad + a_{23}a_{33}(a_{36}a_{41} - a_{35}a_{42}) - a_{24}a_7(a_{36}a_{44} + a_{38}a_{42})\\
&\quad - a_{24}a_{30}(a_{36}a_{43} + a_{14}a_{44} + a_{37}a_{42}) + a_8a_{24}(a_{35}a_{44} + a_{38}a_{41})\\
&\quad + a_{31}a_{24}(a_{35}a_{43} + a_{13}a_{44} + a_{37}a_{41}) - a_{32}a_{24}(a_{36}a_{41} - a_{35}a_{42})\\
&\quad - a_{24}a_{33}(a_{14}a_{41} - a_{13}a_{42}) + a_4a_9(a_{36}a_{44} + a_{38}a_{42})\\
&\quad - a_{29}a_4(a_{36}a_{43} + a_{14}a_{44} + a_{37}a_{42}) + a_4a_8(a_{34}a_{44} - a_{38}a_{40})\\
&\quad + a_4a_{31}(a_{34}a_{43} - a_{15}a_{44} + a_{38}a_{39} - a_{37}a_{40}) + a_4a_{32}(a_{34}a_{42} + a_{36}a_{40})\\
&\quad - a_4a_{33}(a_{15}a_{42} - a_{14}a_{40} + a_{36}a_{39}) - a_5a_9(a_{35}a_{44} + a_{38}a_{41})\\
&\quad + a_5a_{29}(a_{35}a_{43} + a_{13}a_{44} + a_{37}a_{41}) - a_5a_7(a_{34}a_{44} - a_{38}a_{40})\\
&\quad + a_5a_{30}(a_{34}a_{43} - a_{15}a_{44} + a_{38}a_{39} - a_{37}a_{40}) - a_5a_{32}(a_{34}a_{41} + a_{35}a_{40})\\
&\quad + a_5a_{33}(a_{15}a_{41} + a_{35}a_{39} - a_{13}a_{40}) + a_9a_{25}(a_{36}a_{41} - a_{35}a_{42})\\
&\quad + a_{20}a_{26}(a_{36}a_{41} - a_{35}a_{42}) - a_{20}a_{25}(a_{14}a_{41} - a_{13}a_{42})\\
&\quad + a_{30}a_{25}(a_{15}a_{42} + a_{14}a_{39} + a_{36}a_{39} - a_{14}a_{40}) + a_{25}a_8(a_{34}a_{41} + a_{35}a_{40})\\
&\quad - a_{26}a_{31}(a_{35}a_{41} + a_{35}a_{40}) - a_{25}a_{31}(a_{15}a_{41} + a_{35}a_{39} - a_{13}a_{40}),\\
A_5 &= -a_{24}a_{30}(a_{36}a_{44} + a_{38}a_{42}) + a_{24}a_{31}(a_{35}a_{44} + a_{39}a_{42}) - a_{24}a_{33}(a_{36}a_{41} - a_{35}a_{42}) - a_4a_{29}(a_{36}a_{44} + a_{38}a_{42})\\
&\quad + a_{31}a_4(a_{34}a_{44} - a_{38}a_{40}) + a_4a_{33}(a_{34}a_{42} + a_{36}a_{40}) + a_5a_{29}(a_{35}a_{44} + a_{38}a_{41}) - a_5a_{30}(a_{34}a_{44} - a_{38}a_{40})\\
&\quad - a_5a_{33}(a_{35}a_{41} + a_{36}a_{40}) - a_{20}a_{25}(a_{36}a_{41} - a_{35}a_{33}) - a_{25}a_{30}(a_{34}a_{42} + a_{36}a_{40}) + a_{25}a_{31}(a_{34}a_{41} + a_{35}a_{40}),
\end{aligned}
$$

$$R_j^* = \frac{(a_9m_j^2 - a_{29})h_{11} + (a_8m_j^2 + a_{31})h_{12} - (a_{32}m_j^2 + a_{33})h_{13}}{(a_7m_j^2 + a_{30})h_{12} - (a_8m_j^2 + a_{31})h_{14} + (a_{32}m_j^2 + a_{33})h_{15}},$$
$$S_j^* = \frac{(-a_8m_j^2 + a_{29})h_{14} - (a_7m_j^2 + a_{30})h_{12} + (a_{32}m_j^2 + a_{33})h_{16}}{(a_7m_j^2 + a_{30})h_{12} - (a_8m_j^2 + a_{31})h_{14} + (a_{32}m_j^2 + a_{33})h_{15}},$$
$$U_j^* = \frac{(a_9m_j^2 - a_{20})h_{15} - (a_7m_j^2 + a_{30})h_{13} - (a_8m_j^2 + a_{31})h_{16}}{(a_7m_j^2 + a_{30})h_{12} - (a_8m_j^2 + a_{31})h_{14} + (a_{32}m_j^2 + a_{33})h_{15}},$$

$$h_{11} = (a_{14}a_{43}m_j^4 + a_{36}a_{43}m_j^2 + a_{14}a_{43}m_j^2 + a_{36}a_{44} + a_{37}a_{42}m_j^2 + a_{38}a_{42}),$$
$$h_{12} = (-a_{15}a_{43}m_j^4 + a_{34}a_{43}m_j^2 - a_{15}a_{44}m_j^2 + a_{34}a_{44} + a_{37}a_{39}m_j^4 + a_{38}a_{39}m_j^2 - a_{37}a_{40}m_j^2 - a_{38}a_{40}),$$
$$h_{13} = (a_{14}a_{42}m_j^2 - a_{34}a_{42} + a_{14}a_{39}m_j^4 + a_{36}a_{39}m_j^2 - a_{14}a_{40}m_j^2 - a_{36}a_{40}),$$
$$h_{14} = (a_{13}a_{43}m_j^4 + a_{35}a_{43}m_j^2 + a_{13}a_{44}m_j^2 + a_{35}a_{44} + a_{37}a_{41}m_j^2 + a_{38}a_{41}),$$
$$h_{15} = (-a_{13}a_{42}m_j^2 - a_{35}a_{42} + a_{14}a_{41}m_j^2 + a_{36}a_{41}),$$
$$h_{16} = (a_{15}a_{41}m_j^2 - a_{34}a_{41} + a_{13}a_{39}m_j^4 + a_{35}a_{39}m_j^2 - a_{13}a_{40}m_j^2 - a_{35}a_{40}),$$

Appendix II

$$c_{11} = \frac{\lambda}{\beta_1 T_0}, \quad c_{12} = \frac{\mu}{\beta_1 T_0}, \quad c_{13} = \frac{b\alpha_1}{\varphi_1 \omega^{*2} \beta_1 T_0}, \quad c_{14} = \frac{d\alpha_1}{\varphi_1 \omega^{*2} \beta_1 T_0},$$
$$c_{15} = \frac{\alpha}{4} \frac{\omega^{*2}}{\beta_1 T_0 c_1^2}, \quad c_{16} = \frac{\alpha_1}{\omega^{*2} \varphi_1}, \quad c_{17} = \frac{b_1 \alpha_1}{\omega^{*2} \alpha \varphi_1}, \quad c_{18} = \frac{\gamma_0 \alpha_1}{\alpha \varphi_1 \omega^{*2}}.$$

Appendix III

$$Q_j^0 = c_{11}m_j^2 + c_{12}(m_j^2 - k^2) + c_{13}R_j^* + c_{14}S_j^* - [1 + \zeta^*(m_j^2 - k^2)]U_j^*,$$
$$H_j^0 = 2ikc_{12}m_j,$$
$$N_j^0 = c_{16}m_jR_j^* + c_{17}m_jS_j^*,$$
$$E_j^0 = c_{17}m_jR_j^* + c_{18}m_jS_j^*,$$
$$L_j^0 = (m_j^2 - k^2), \quad j = 1, 2, 3, 4.$$
$$Q_j^0 = -2ikc_{12}m_j,$$
$$H_j^0 = [c_{12}(m_j^2 + k^2) + c_{15}(m_j^2 - k^2)^2],$$
$$M_j^0 = (m_j^2 - k^2), \quad j = 5, 6.$$